Proceedings of the
44th IEEE Conference on Decision and Control, and
the European Control Conference 2005
Seville, Spain, December 12-15, 2005

Leader/Follower synchronization of satellite attitude without angular velocity measurements

Anne Karin Bondhus, Kristin Y. Pettersen and J. Tommy Gravdahl
Department of Engineering Cybernetics, Norwegian University of Science and Technology
N-7491 Trondheim, Norway

Abstract— **In this paper we propose a Leader/Follower output feedback synchronization scheme for control of the attitude of two satellites when angular velocity measurements are not available. Nonlinear observers are used to estimate the angular velocities. The attitudes of the satellites are represented by unit quaternions, and the control design is based on vectorial observer backstepping. The analysis of the method shows that the rotation matrices representing the attitude errors between the follower and the leader, and between the leader and its reference attitude, converge to the identity matrix for any initial conditions. The control scheme is simulated to validate the results.**

I. INTRODUCTION

Formation flying of satellites introduces several advantages compared to single spacecraft missions. These include increased flexibility, distributed functionality, lowered total cost and risk, and redundancy. Precise formation flying of satellites and other spacecraft makes applications such as large-scale distributed sensing (radar, interferometry, imaging etc.) possible. On the other hand, the advantages of using multiple spacecraft in formation comes at a cost of increased complexity, and introduces the need for simultaneous launch, configuration initialization and coordinated control. The topic of this paper is formation attitude control. The literature in the field of spacecraft formation flying control has to a large extent focused on the relative position control problem, see [1] for an extensive overview, however notable exceptions exist.

State Feedback Tracking: In [2] and [3] nearest neighbour full state feedback tracking control laws to maintain relative position and attitude between several spacecraft in a formation were developed. Exponential stability was proved. [4] propose a coordination architechture for spacecraft formation flying that includes Leader/Follower as a special case. The control problem is solved as a tracking problem and global convergence is proven. A similar result for attitude control of a single spacecraft is found in [5]. In [6], a globally convergent adaptive control law for a follower spacecraft tracking both position and orientation of a leader spacecraft assuming full state knowledge of both craft but no knowledge of mass and inertia is derived.

Output Feedback Tracking: [7] presents a globally convergent output feedback attitude tracking control law without angular velocity measurements for a single spacecraft and in [8] an output feedback controller for control of the relative positions of a formation of spacecraft is presented. Based on the results of [9], [10] derived a convergent scheme for tracking of attitude and formation keeping for multiple spacecrafts in a formation where information flows in a bidirectional ring structure.

Note that if tracking by state or output feedback is used for coordinated attitude control of a formation of satellites, the coordination is made at the trajectory planning level. The reference attitude trajectories are chosen such that the satellite motion is coordinated if all the satellites are able to follow their reference trajectory accurately. Disturbances may however prevent the satellites from following their reference trajectories precisely. A synchronization control scheme copes with this by controlling the relative errors between some or all of the satellite attitudes in a more direct manner.

Syncronization: Using a framework similar to that of [11] for formation position control, [12] proposes a scheme for coordinated attitude control by state feedback for the case where the leader satellite is not able to follow its reference attitude trajectory due to environmental disturbances. A reference projection is proposed, so that the follower satellite is commanded to follow a combination of its reference attitude and the measured or communicated leader satellite attitude.

In this paper we propose a Leader/Follower output feedback synchronization scheme for control of the attitude of two satellites when angular velocity measurements are not available. Instead of designing reference trajectories for each satellite, the coordination of the two satellites is made directly in the control law. The attitude of the follower satellite should track the attitude of the leader satellite, i. e. the relative error is controlled directly. The attitude of the leader system, on the other hand, should track any time-varying reference attitude, which is typically given mathematically. When the leader satellite is subjected to disturbances, controlling the relative error directly may give smaller relative errors than traditional tracking control .

It is assumed that attitude is measured using sensors such as startracker, sun sensor, earth sensor, magnetometer, GPS or a combination of these. We assume that angular velocity measurement is not present. The motivation for avoiding rate gyros is that they are expensive, failure-prone, heavy and use a significant amount of power [13]. If gyros are present for angular velocity measurement, the angular rate estimate is still useful as backup or in case of failure of equipment. The attitude determination and control system (ADCS) of most satellites includes an observer, usually an extended Kalman

0-7803-9568-9/05/$20.00 ©2005 IEEE

filter (EKF), and the observer in the present paper is regarded as part of such a system.

Based on vectorial observer backstepping we develop an output feedback synchronization control scheme that gives asymptotic stability of the Leader/Follower system. For attitude synchronization of a formation of many satellites, one may use one satellite as the leader and apply Leader/Follower synchronization between the leader and each of the other satellites.

The paper is organized as follows. In Sec. II notation and preliminaries are given. Sec. III presents the system equations, and Sec. IV describes the control objective. In section V the type of observer used in the synchronization scheme is presented, and the special observer used for the simulations in this paper is described. Sec. VI presents the main result of the paper, which is the controller design method for output synchronization and tracking. Section VII presents an analysis of the transient response. Simulations are presented in Sec. VIII in order to validate the results.

II. PRELIMINARIES

This section describes the notation for rotation matrices, unit quaternions and angular velocities, and some of their properties used in this paper. In addition the kinematic differential equations for rotation matrices and quaternions are presented [14], [15]. The attitude of system b relative to system a is given by the rotation matrix $\mathbf{R}_b^a$ with columns equal to the basis vectors of system b decomposed in the a-frame. For the attitude relative to the inertial system the upper index is not used, i. e. $\mathbf{R}_b := \mathbf{R}_b^i$, where i is the inertial system. In this paper rotation matrices will be parameterized in terms of unit quaternions. The representation in terms of quaternions is a 4-parameter singularity-free representation, as opposed to 3-parameter representations, which cannot be used for all attitudes because of singularities. Therefore the representation in terms of quaternions is much used for systems where large rotations may occur, for example for satellites. According to Euler's theorem on rotation, the rotation of system b relative to system a can be given as a rotation through an angle θ about an axis $\mathbf{k}$. The unit quaternion that represents the rotation matrix $\mathbf{R}_b^a$ is defined by a real part $\eta := \cos\frac{\theta}{2}$ and an imaginary part, vector part, $\boldsymbol{\epsilon}^T = [\ \epsilon_1 \quad \epsilon_2 \quad \epsilon_3\ ] := \sin\frac{\theta}{2}\mathbf{k}^T$.

The rotation matrix is then given by

$$\mathbf{R}_b^a(\mathbf{q}) = \mathbf{I}_{3\times 3} + 2\eta\mathbf{S}(\boldsymbol{\epsilon}) + 2\mathbf{S}^2(\boldsymbol{\epsilon}) \qquad (1)$$

Both $\mathbf{q}$ and $-\mathbf{q}$ give the same rotation matrix.

It can be shown that $\mathbf{R}_c^a = \mathbf{R}_b^a\mathbf{R}_c^b$. A general relation on this form is $\mathbf{R} = \mathbf{R}_1\mathbf{R}_2$ where the quaternion for $\mathbf{R}_1$ is $\mathbf{q}_1^T = [\ \eta_1 \quad \boldsymbol{\epsilon}_1^T\ ]$ and the quaternion for $\mathbf{R}_2$ is $\mathbf{q}_2^T = [\ \eta_2 \quad \boldsymbol{\epsilon}_2^T\ ]$. The quaternion $\mathbf{q}$ for $\mathbf{R}$ is then $\mathbf{q} = \mathbf{q}_1 \otimes \mathbf{q}_2$, where $\otimes$ denotes quaternion multiplication defined by

$$\mathbf{q}_1 \otimes \mathbf{q}_2 := \begin{bmatrix} \eta_1 & -\boldsymbol{\epsilon}_1^T \\ \boldsymbol{\epsilon}_1 & \eta_1\mathbf{I} + \mathbf{S}(\boldsymbol{\epsilon}_1) \end{bmatrix} \begin{bmatrix} \eta_2 \\ \boldsymbol{\epsilon}_2 \end{bmatrix} \qquad (2)$$

and $\mathbf{S}(\mathbf{x})$ is the skew-symmetric cross-product operator matrix such that $\mathbf{x}_1 \times \mathbf{x}_2 = \mathbf{S}(\mathbf{x}_1)\mathbf{x}_2$.

The inverse of $\mathbf{q}_1$ is $\mathbf{q}_1^{-1} = [\ \eta_1 \quad -\boldsymbol{\epsilon}_1^T\ ]^T$, and satisfies $\mathbf{q}_1^{-1} \otimes \mathbf{q}_1 = \mathbf{q}_1 \otimes \mathbf{q}_1^{-1} = \mathbf{1}_q$, where $\mathbf{1}_q := [\ 1 \quad \mathbf{0}^T\ ]^T$ is the identity quaternion. This gives that

$$\mathbf{q}_2 = \mathbf{q}_1 \otimes \tilde{\mathbf{q}} \Leftrightarrow \tilde{\mathbf{q}} = \mathbf{q}_1^{-1} \otimes \mathbf{q}_2 \qquad (3)$$

The angular velocity of system b relative to system a will be denoted $\boldsymbol{\omega}_{ab}^k$, where the upper index k denotes the frame in which the angular velocity is decomposed.

It can be shown that in terms of the rotation matrix the kinematic differential equation is

$$\dot{\mathbf{R}}_b^a = \mathbf{S}(\boldsymbol{\omega}_{ab}^a)\mathbf{R}_b^a = \mathbf{R}_b^a\mathbf{S}(\boldsymbol{\omega}_{ab}^b) \qquad (4)$$

and written in terms of the quaternion $\mathbf{q}$ that represents $\mathbf{R}_b^a$ it is

$$\dot{\mathbf{q}} = \frac{1}{2}[\boldsymbol{\omega}_{ab}^a]_q \otimes \mathbf{q} = \frac{1}{2}\mathbf{q} \otimes [\boldsymbol{\omega}_{ab}^b]_q \qquad (5)$$

For an angular velocity $\boldsymbol{\omega}$ we define $[\boldsymbol{\omega}]_q$ as the quaternion with real part equal to 0 and imaginary part equal to $\boldsymbol{\omega}$.

It can be shown that

$$\boldsymbol{\omega}_{ab}^k = \boldsymbol{\omega}_{ib}^k - \boldsymbol{\omega}_{ia}^k \qquad (6)$$

for representation in any frame k.

For a reference attitude $\mathbf{q}_d(t)$ given mathematically, $\dot{\mathbf{q}}_d$ and higher order derivatives can be calculated by direct differentiation of the expression for $\mathbf{q}_d$. The angular velocity $\boldsymbol{\omega}_{id}^i$ of $\mathbf{q}_d$ can be calculated from $\mathbf{q}_d$ and $\dot{\mathbf{q}}_d$. From

$$\dot{\mathbf{q}}_d = \frac{1}{2}[\boldsymbol{\omega}_{id}^i]_q \otimes \mathbf{q}_d \qquad (7)$$

it is found by quaternion multiplication on the right with $2\mathbf{q}_d^{-1}$ on both sides that

$$[\boldsymbol{\omega}_{id}^i]_q = 2\dot{\mathbf{q}}_d \otimes \mathbf{q}_d^{-1} \qquad (8)$$

The real part of the calculation in (8) is necessarily because $|\mathbf{q}_d| = 1$, and the vector part of the result is equal to $\boldsymbol{\omega}_{id}^i(t)$.

We define the following quaternions for use in the tracking/synchronization scheme to give rotations relative to the inertial system:

$$\begin{array}{lll} \mathbf{q}_d & : & \text{Desired attitude of the leader.} \\ \mathbf{q}_l & : & \text{Attitude of the leader.} \\ \mathbf{q}_f & : & \text{Attitude of the follower.} \\ \hat{\mathbf{q}}_l & : & \text{Estimated attitude of the leader.} \\ \hat{\mathbf{q}}_f & : & \text{Estimated attitude of the follower.} \end{array} \qquad (9)$$

It will be implied that for any index k the matrix $\mathbf{R}_k$ is the rotation matrix corresponding with $\mathbf{q}_k$, and $\hat{\mathbf{R}}_k$ corresponds with $\hat{\mathbf{q}}_k$.

The error quaternions are defined according to (3) and are given by

$$\begin{array}{ll} \mathbf{e}_l := \mathbf{q}_d^{-1} \otimes \mathbf{q}_l & \hat{\mathbf{e}}_l := \mathbf{q}_d^{-1} \otimes \hat{\mathbf{q}}_l \\ \mathbf{e}_f := \mathbf{q}_l^{-1} \otimes \mathbf{q}_f & \hat{\mathbf{e}}_f := \hat{\mathbf{q}}_l^{-1} \otimes \hat{\mathbf{q}}_f \\ \tilde{\mathbf{q}}_l := \mathbf{q}_l^{-1} \otimes \hat{\mathbf{q}}_l & \tilde{\mathbf{q}}_f := \mathbf{q}_f^{-1} \otimes \hat{\mathbf{q}}_f \end{array} \qquad (10)$$

The error quaternions are illustrated in Fig. 1. They are all unit quaternions, i.e. have length one.

For any measurable function $\mathbf{u} : [0,\infty\rangle \to \mathbb{R}^n$ we define

$$||\mathbf{u}||_\infty := \sup_{t\in[0,\infty\rangle} |\mathbf{u}(t)| \qquad ||\mathbf{u}||_a := \limsup_{t\to\infty} |\mathbf{u}(t)| \qquad (11)$$

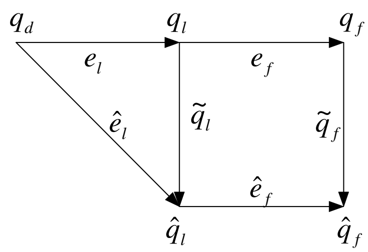

Fig. 1. Illustration of quaternion error variables

where each supremum is understood to be an essential supremum. The norm $||\mathbf{u}||_\infty$ is referred to as the $\mathcal{L}_\infty$-norm of $\mathbf{u}$, while $||\mathbf{u}||_a$ is referred to as the asymptotic $\mathcal{L}_\infty$-norm of $\mathbf{u}$. The initial value of a variable or function x will be denoted x_0.

III. System equations

The system equations are given by the kinematic differential equation (5) together with the dynamical equation:

$$\dot{\mathbf{q}}_k = \frac{1}{2}[\boldsymbol{\omega}_{ik}^i]_q \otimes \mathbf{q}_k \tag{12}$$

$$\frac{d}{dt}(\mathbf{J}_k^i \boldsymbol{\omega}_{ik}^i) = \boldsymbol{\tau}_k^i \tag{13}$$

where $k = l$ for the leader and $k = f$ for the follower. The last equation is the dynamics as seen from the inertial system, with $\mathbf{J}_k^i = \mathbf{R}_k \mathbf{J}_k^k \mathbf{R}_k^T$ where $\mathbf{J}_k^k$ is the inertia matrix calculated in the k-frame, see [15]. Since the system does not move in the k-frame $\mathbf{J}_k^k$ is constant. It can be shown that $\mathbf{J}_k^k$ and $\mathbf{J}_k^i$ are symmetric and positive definite. The control is $\boldsymbol{\tau}_k^i$.

The output of the system is $\mathbf{q}_k$, since it is assumed that the attitude is measured, whereas measurement of the angular velocity $\boldsymbol{\omega}_{ik}^i$ is assumed to be unavailable (see the Introduction).

IV. Control objective

The objective of the tracking/synchronization control is to design $\boldsymbol{\tau}_f^i$ and $\boldsymbol{\tau}_l^i$ by output feedback control such that (12-13) for $k = l$ and $k = f$ together with the observer dynamics presented in the next section give asymptotic convergence of $\mathbf{q}_l$ to $\mathbf{q}_d$, and of $\mathbf{q}_f$ to $\mathbf{q}_l$.

We will call the problem of getting $\mathbf{q}_l$ to track $\mathbf{q}_d$ "the tracking problem", while the problem of getting $\mathbf{q}_f$ to track $\mathbf{q}_l$ will be called "the synchronization problem". These problems are different, because for the tracking problem the desired trajectory $\mathbf{q}_d$ is given mathematically, while for the synchronization problem the desired trajectory is $\mathbf{q}_l$, which is a measured trajectory. For $\mathbf{q}_d$ all higher order derivatives can be calculated, and from this the angular velocity $\boldsymbol{\omega}_{id}^i$ of $\mathbf{q}_d$ and all higher order derivatives of the angular velocity can be found. On the other hand, the angular velocity $\boldsymbol{\omega}_{il}^i$ of the desired trajectory in the synchronization problem is unavailable. This adds an extra difficulty to the problem, and implies that in the synchronization problem an observer must be used to estimate the angular velocity of the desired trajectory. In addition comes that the angular velocity of the follower itself is not measured, such that we need an observer for this as well. The problem is thus an output feedback synchronization control problem. Also, since the angular velocity of the leader is not available, the problem of getting $\mathbf{q}_l$ to track $\mathbf{q}_d$ is an output feedback tracking control problem. Although there are differences between the tracking and synchronization problem the controller for both problems will be designed in a similar manner by the control design method presented in this paper.

The control objective is therefore to use angular velocity observers and find control laws

$$\boldsymbol{\tau}_l^i = \boldsymbol{\tau}_l^i(\mathbf{q}_d, \boldsymbol{\omega}_{id}^i, \dot{\boldsymbol{\omega}}_{id}^i, \ldots, \mathbf{q}_l, \hat{\mathbf{q}}_l, \hat{\boldsymbol{\omega}}_{il}^i) \tag{14}$$

$$\boldsymbol{\tau}_f^i = \boldsymbol{\tau}_f^i(\mathbf{q}_l, \hat{\mathbf{q}}_l, \hat{\boldsymbol{\omega}}_{il}^i, \mathbf{q}_f, \hat{\mathbf{q}}_f, \hat{\boldsymbol{\omega}}_{if}^i) \tag{15}$$

such that $\mathbf{e}_l \to \pm\mathbf{1}_q$ and $\mathbf{e}_f \to \pm\mathbf{1}_q$, which implies $\mathbf{q}_l \to \mathbf{q}_d$ and $\mathbf{q}_f \to \mathbf{q}_l$. In (14-15) $\hat{\boldsymbol{\omega}}_{ik}^i$ for $k = l$ or $k = f$ is the estimate of the angular velocity. The dots in (14) indicate that derivatives of any order may be used. However, we will not use derivatives of higher order than $\dot{\boldsymbol{\omega}}_{id}^i$. In Fig. 2 the structure of the system is shown. The input $\mathbf{a}_D$ to the follower observer will be a function of the other variables and is therefore not included in (15).

V. Angular velocity nonlinear observer

In this section the observer used to estimate the angular velocities of the systems is presented. A nonlinear observer for estimation of angular velocity for rigid body motion was presented in [16]. This observer was modified in [17] in order to include different types of correction terms in the observer, and to give the error quaternion between system a and b in the a-coordinates instead of in the inertial coordinates as in [16]. We consider observers that have the following structure

$$\dot{\hat{\mathbf{q}}}_k = \frac{1}{2}[\hat{\boldsymbol{\omega}}_{ik}^i + \mathbf{g}_{1k}] \otimes \hat{\mathbf{q}}_k \tag{16}$$

$$\frac{d}{dt}(\mathbf{J}_k^i \hat{\boldsymbol{\omega}}_{ik}^i) = \boldsymbol{\tau}_k^i + \mathbf{g}_{2k} \tag{17}$$

where $k = l$ for the leader and $k = f$ for the follower.

In the simulations we apply the observer presented in [17, Sec. 6.2], which has the form in (16-17) with

$$\mathbf{g}_{1k}(\mathbf{q}_k, \mathbf{z}_k) := -\mathbf{K}_{v,k}\mathbf{R}_k\mathbf{z}_k \tag{18}$$

$$\mathbf{g}_{2k}(\mathbf{q}_k, \mathbf{z}_k) := -\frac{1}{2}k_{p,k}(\mathbf{J}_k^i)^{-1}\mathbf{R}_k\mathbf{z}_k = -\frac{1}{2}k_{p,k}\mathbf{R}_k(\mathbf{J}_k^k)^{-1}\mathbf{z}_k \tag{19}$$

and

$$\mathbf{z}_k = -\frac{dH}{d\tilde{\eta}_k}\tilde{\boldsymbol{\epsilon}}_k \tag{20}$$

where $k_{p,k}$ is a positive scalar, $\mathbf{K}_{v,k} = \mathbf{K}_{v,k}^T > 0$. The observer error is $\tilde{\mathbf{q}}_k^T = [\ \tilde{\eta}_k \quad \tilde{\boldsymbol{\epsilon}}_k^T\ ]$..

In [17] general properties that H must satisfy are given, and different choices for H are presented. One of the choices is

$$H(\tilde{\eta}_k) = \begin{cases} 1 + \tilde{\eta}_k & \text{for } \tilde{\eta}_k < 0 \\ 1 - \tilde{\eta}_k & \text{for } \tilde{\eta}_k \geq 0 \end{cases} \tag{21}$$

$$\Rightarrow \mathbf{z}_k = \operatorname{sgn}(\tilde{\eta}_k)\tilde{\boldsymbol{\epsilon}}_k \tag{22}$$

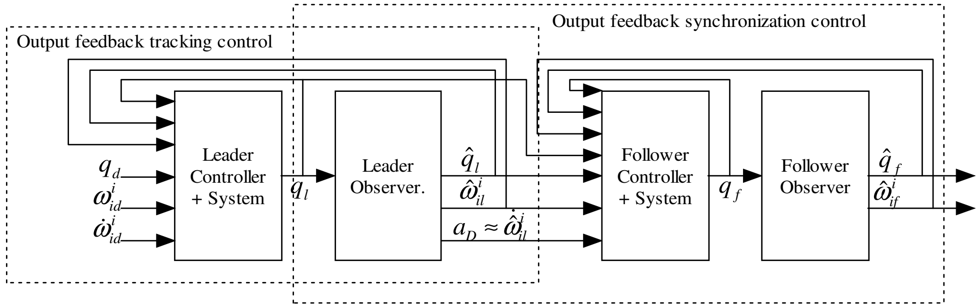

Fig. 2. Leader-follower synchronization of attitude

where

$$\text{sgn}(\tilde{\eta}_k) = \begin{cases} -1 \text{ for } \tilde{\eta}_k < 0 \\ +1 \text{ for } \tilde{\eta}_k \geq 0 \end{cases} \tag{23}$$

which is the function used in the simulations in this paper. It is important to define the sgn-function as in (23), and not such that $\text{sgn}(0) = 0$ as this would lead to an extra equilibrium point for $\tilde{\eta}_k = 0$.

In [17, Sec. 6.2.1] a stability result was deduced for the use of any H-function with specified properties. We here state the theorem only for the H-function used in this paper:

Theorem 1: If the observer given by (16-21) with $\mathbf{g}_{1k}$ and $\mathbf{g}_{2k}$ defined by (18-19), is applied to the system (12-13), it can be concluded that for any initial values of the attitude error and angular velocity error, $\tilde{\mathbf{q}}_k \to \pm\mathbf{1}_q$, which implies that $\tilde{\mathbf{R}}_k$ converges asymptotically to $\mathbf{I}$, and $\tilde{\boldsymbol{\omega}}_{ik}^i := (\hat{\boldsymbol{\omega}}_{ik}^i - \boldsymbol{\omega}_{ik}^i) \to 0$.

From (16) it can be seen that the angular velocity of the estimated system is given by

$$\boldsymbol{\omega}_{i\hat{k}}^i = \hat{\boldsymbol{\omega}}_{ik}^i + \mathbf{g}_{1k} \tag{24}$$

Notice that the estimated angular velocity $\hat{\boldsymbol{\omega}}_{ik}^i$ is not equal to the angular velocity of the estimated system.

The control design presented in this paper may be used for any observer on the form (16-17). In the control design the only assumption about the observer will be

Assumption 1: The observer is in the form (16-17), where the observer terms $\mathbf{g}_{1k}$, $\mathbf{g}_{2k}$ are any expressions such that for any angular velocity of the observed trajectory, it can be shown that the observer errors are bounded, $\tilde{\mathbf{q}}_k \to \pm\mathbf{1}_q$ and $\tilde{\boldsymbol{\omega}}_{ik}^i \to 0$. This implies that $\mathbf{g}_{1k}$ and $\mathbf{g}_{2k}$ will converge to zero, since the observer dynamics must be equal to the actual dynamics after convergence of the observer errors.

VI. CONTROLLER DESIGN

A. Design method

We propose a controller design based on vectorial observer backstepping [18], [19], in which backstepping design is applied to the observer equations. In [18] vectorial observer backstepping was applied to the design of nonlinear output feedback control of dynamically positioned ships. In [20] some comments to [18] were given in order to enlarge the method to a larger class of ships. In [21] a sliding mode observer (with the saturation function) was developed for a ship, and the vectorial observer backstepping method was used to design the control input. In [22] a controller for attitude based on backstepping was developed, with full state feedback and for rest-to-rest maneuver.

We choose $\hat{\mathbf{e}}_l$ and $\hat{\mathbf{e}}_f$ as error dynamics coordinates, and the controllers will be designed such that $\hat{\mathbf{e}}_l$ and $\hat{\mathbf{e}}_f$ converge to $\pm\mathbf{1}_q$ if an observer satisfying Ass. 1 is used. Another alternative would be to use $\mathbf{e}_l$ and $\mathbf{e}_f$ as error coordinates instead, but it was found that the use of $\hat{\mathbf{e}}_l$ and $\hat{\mathbf{e}}_f$ lead to simpler design of the controller. For instance, the term (**??**) could not be calculated exactly if $\mathbf{e} := \mathbf{e}_1$ or $\mathbf{e} := \mathbf{e}_f$ because the angular velocity of $\mathbf{e}$ would then be unknown.

From Fig. 1 it is seen that if $\hat{\mathbf{e}}_l$, $\hat{\mathbf{e}}_f$, $\tilde{\mathbf{q}}_l$ and $\tilde{\mathbf{q}}_f$ converge to $\pm\mathbf{1}_q$ also $\mathbf{e}_l$ and $\mathbf{e}_f$ converge to $\pm\mathbf{1}_q$. This implies that $\mathbf{q}_l \to \mathbf{q}_d$ and $\mathbf{q}_f \to \mathbf{q}_l$, which is the objective of the controller design.

B. Error dynamics for the tracking/synchronization errors

This section presents the differential equations for $\hat{\mathbf{e}}_l$ and $\hat{\mathbf{e}}_f$. From (5) and (6) it can be seen that the differential equation for $\hat{\mathbf{e}}_l$ is given by

$$\begin{aligned}\dot{\hat{\mathbf{e}}}_l &= \frac{1}{2}[\boldsymbol{\omega}_{i\hat{l}}^d - \boldsymbol{\omega}_{id}^d]_q \otimes \hat{\mathbf{e}}_l \\ &= \frac{1}{2}[\mathbf{R}_d^T(\boldsymbol{\omega}_{i\hat{l}}^i - \boldsymbol{\omega}_{id}^i)]_q \otimes \hat{\mathbf{e}}_l\end{aligned} \tag{25}$$

By inserting for $\boldsymbol{\omega}_{i\hat{l}}^i$ from (24) with $k = l$ (25) becomes

$$\dot{\hat{\mathbf{e}}}_l = \frac{1}{2}[\mathbf{R}_d^T(\hat{\boldsymbol{\omega}}_{il}^i - \boldsymbol{\omega}_{id}^i + \mathbf{g}_{1l})]_q \otimes \hat{\mathbf{e}}_l \tag{26}$$

Similarly the differential equation for $\hat{\mathbf{e}}_f$ can be written as

$$\begin{aligned}\dot{\hat{\mathbf{e}}}_f &= \frac{1}{2}[\boldsymbol{\omega}_{i\hat{f}}^{\hat{l}} - \boldsymbol{\omega}_{i\hat{l}}^{\hat{l}}]_q \otimes \hat{\mathbf{e}}_f \\ &= \frac{1}{2}[\hat{\mathbf{R}}_l^T(\hat{\boldsymbol{\omega}}_{if}^i - \hat{\boldsymbol{\omega}}_{il}^i + \mathbf{g}_{1f} - \mathbf{g}_{1l})]_q \otimes \hat{\mathbf{e}}_f\end{aligned} \tag{27}$$

The differential equations for $\hat{\mathbf{e}}_l$ and $\hat{\mathbf{e}}_f$ are similar, except that $\hat{\mathbf{e}}_l$ is only influenced by the observer error for the leader-observer, while $\hat{\mathbf{e}}_f$ is influenced by the observer errors of both the observer for the leader satellite and the observer for the follower satellite. It is assumed that the observers satisfy Ass. 1. Since no assumptions about the trajectory to be observed is necessary for the observer, there is no coupling between the observer dynamics and tracking dynamics as was the case for synchronization of robots in [23]. The observer errors, and therefore $\mathbf{g}_{1f}$ and $\mathbf{g}_{1l}$, can be treated as inputs to (26) and (27) with given bounds, and according to Ass. 1 $\mathbf{g}_{1f} \to 0$ and $\mathbf{g}_{1l} \to 0$.

C. The controllers

By using the equations (17), (26-27) we are able to design the output tracking controller for the leader and the output synchronization controller for the follower in a similar manner using vectorial observer backstepping. Both (26) and (27) are in the form

$$\dot{\mathbf{e}} = \frac{1}{2}[\mathbf{R}_1^T(\hat{\boldsymbol{\omega}} - \boldsymbol{\omega}_D + \mathbf{v}_O)]_q \otimes \mathbf{e} \tag{28}$$

with (17) in the form

$$\frac{d}{dt}(\mathbf{J}\hat{\boldsymbol{\omega}}) = \boldsymbol{\tau} + \mathbf{g}_2 \tag{29}$$

For the output feedback tracking problem of the leader system (28) represents (26). This implies that $\mathbf{e} = \hat{\mathbf{e}}_l$, $\mathbf{R}_1 = \mathbf{R}_d$, $\hat{\boldsymbol{\omega}} = \hat{\boldsymbol{\omega}}_{il}^i$, $\boldsymbol{\omega}_D = \boldsymbol{\omega}_{id}^i$ and $\mathbf{v}_O = \mathbf{g}_{1m}$. For the problem of output feedback synchronizing of the follower (28) represents (27). In this case $\mathbf{e} = \hat{\mathbf{e}}_f$, $\mathbf{R}_1 = \hat{\mathbf{R}}_l$, $\hat{\boldsymbol{\omega}} = \hat{\boldsymbol{\omega}}_{if}^i$, $\boldsymbol{\omega}_D = \hat{\boldsymbol{\omega}}_{il}^i$ and $\mathbf{v}_O = \mathbf{g}_{1f} - \mathbf{g}_{1l}$.

The term $\mathbf{v}_O$ is a disturbance term caused by the observer errors. For both problems there is a bound for $|\mathbf{v}_O|$ from the analysis of the observer, and $\mathbf{v}_O$ goes to 0 as the observer errors go to zero.

Equation (29) represents the observer equation (17). This gives that $\mathbf{J} := \mathbf{J}_k^i$, $\hat{\boldsymbol{\omega}} := \hat{\boldsymbol{\omega}}_{ik}^i$, $\boldsymbol{\tau} = \boldsymbol{\tau}_k^i$ and $\mathbf{g}_2 = \mathbf{g}_{2k}$ where $k = l$ for the tracking problem of the leader and $k = f$ for the synchronization problem. We also define $\mathbf{J}_0 = \mathbf{J}_k^k$, such that $\mathbf{J} = \mathbf{R}_k\mathbf{J}_0\mathbf{R}_k^T$.

A difference between the tracking problem and the synchronization problem is that while for the tracking problem $\dot{\boldsymbol{\omega}}_D$ can be accurately calculated, this is not the case for the synchronization problem. For the synchronization of the follower to the leader $\dot{\boldsymbol{\omega}}_D = \dot{\hat{\boldsymbol{\omega}}}_{il}^i$. However, from the observer equations for the leader system only $\frac{d}{dt}(\mathbf{J}_l^i\hat{\boldsymbol{\omega}}_{il}^i) = \boldsymbol{\tau}_l^i + \mathbf{g}_{2l}$ is known, and from this it is not possible to calculate $\dot{\hat{\boldsymbol{\omega}}}_{il}^i$, because this requires knowledge of $\dot{\mathbf{J}}_l^i$ that cannot be calculated since it depends on $\boldsymbol{\omega}_{il}^i$.

Using the idea of vectorial observer backstepping design we choose $\hat{\boldsymbol{\omega}}$ as a virtual control for (28), and design $\boldsymbol{\tau}$ such that $\hat{\boldsymbol{\omega}}$ converges towards a desired reference for the virtual control. Let $\hat{\boldsymbol{\omega}}_r$ be the desired ideal value for $\hat{\boldsymbol{\omega}}$, and define the tracking error for $\hat{\boldsymbol{\omega}}$ as

$$\mathbf{s} = \hat{\boldsymbol{\omega}} - \hat{\boldsymbol{\omega}}_r \Rightarrow \hat{\boldsymbol{\omega}} = \hat{\boldsymbol{\omega}}_r + \mathbf{s} \tag{30}$$

By inserting (30) into (28) the dynamics of $\mathbf{e}$ become

$$\dot{\mathbf{e}} = \frac{1}{2}[\mathbf{R}_1^T(\hat{\boldsymbol{\omega}}_r - \boldsymbol{\omega}_D + \mathbf{s} + \mathbf{v}_O)]_q \otimes \mathbf{e} \tag{31}$$

We define the reference trajectory as

$$\hat{\boldsymbol{\omega}}_r = \mathbf{R}_1\boldsymbol{\alpha}_1(\mathbf{e}) + \boldsymbol{\omega}_D \tag{32}$$

where $\boldsymbol{\alpha}_1(\mathbf{e})$ is defined later. The definition of $\hat{\boldsymbol{\omega}}_r$ implies that (31) becomes

$$\dot{\mathbf{e}} = \frac{1}{2}[\boldsymbol{\alpha}_1(\mathbf{e}) + \mathbf{R}_1^T(\mathbf{s} + \mathbf{v}_O)]_q \otimes \mathbf{e} \tag{33}$$

In Section VII the dynamics in (33) is analysed and possible choices of $\boldsymbol{\alpha}_1(\mathbf{e})$ are given such that $\mathbf{e} \to \pm\mathbf{1}_q$ if $|\mathbf{s}|$,$|\mathbf{v}_O|$ are bounded and $\mathbf{s}, \mathbf{v}_O \to 0$ as $t \to 0$.

We assume that $\boldsymbol{\alpha}_1(\mathbf{e})$ is defined as in Section VII. The aim of the control design is then to find a control such that the dynamics of $\mathbf{s}$ is asymptotically stable. The dynamics of $\mathbf{v}_O$ is asymptotically stable as shown by the observer analysis.

If $\frac{d}{dt}(\mathbf{J}\hat{\boldsymbol{\omega}}_r)$ was exactly known we could define the control as

$$\boldsymbol{\tau}_{\text{ideal}} = -\mathbf{g}_2 + \frac{d}{dt}(\mathbf{J}\hat{\boldsymbol{\omega}}_r) - \mathbf{A}_s\mathbf{J}\mathbf{s} \tag{34}$$

with $\mathbf{A}_s = \mathbf{A}_s^T > 0$. From (29) it is seen that the closed loop system would then be

$$\frac{d}{dt}(\mathbf{J}\mathbf{s}) = -\mathbf{A}_s\mathbf{J}\mathbf{s} \tag{35}$$

which would give convergence to zero of $\mathbf{J}\mathbf{s}$, and therefore of $\mathbf{s}$, since $\mathbf{J}$ is non-singular. However, $\frac{d}{dt}(\mathbf{J}\hat{\boldsymbol{\omega}}_r)$ is unknown, both for the tracking problem and the synchronization problem, since $\dot{\mathbf{J}}$ is unknown. For the synchronization problem also $\dot{\hat{\boldsymbol{\omega}}}_r$ is unknown. It is therefore difficult to design a controller such that $\mathbf{s} \to 0$ no matter what the observer errors are. We therefore design a controller such that the dynamics of $\mathbf{s}$ depend on the observer errors, but still $\mathbf{s} \to 0$ as $t \to \infty$, under Ass. 1 for the observer. This will be done by finding an approximation to the expression in (34) such that the approximation error go to zero as the observer errors converge.

We propose to use an approximation $\dot{\boldsymbol{\omega}}_D \approx \mathbf{a}_D$ in the synchronization problem, where the expression for $\mathbf{a}_D$ is given in the Appendix. The approximation is such that

$$\dot{\boldsymbol{\omega}}_D = \mathbf{a}_D + \boldsymbol{\delta}_D \tag{36}$$

where the approximation error $\boldsymbol{\delta}_D$ goes to zero as $\tilde{\boldsymbol{\omega}}_{il}^i$ goes to zero. To use the same equations for both the tracking problem and the synchonization problem we define $\boldsymbol{\delta}_D = 0$ and $\mathbf{a}_D = \dot{\boldsymbol{\omega}}_D := \dot{\boldsymbol{\omega}}_{id}^i$ for the tracking problem.

By differentiating (32) and using (36) it is seen that

$$\dot{\hat{\boldsymbol{\omega}}}_r = \mathbf{a}_r + \boldsymbol{\delta}_D \text{ with } \mathbf{a}_r = \frac{d}{dt}(\mathbf{R}_1\boldsymbol{\alpha}_1(\mathbf{e})) + \mathbf{a}_D \tag{37}$$

where $\mathbf{a}_r$ is known, since $\mathbf{a}_D$ and the angular velocity of $\mathbf{R}_1$, $\dot{\mathbf{e}}$ are known.

From (62-63) we get

$$\frac{d}{dt}(\mathbf{J}\hat{\boldsymbol{\omega}}_r) = \mathbf{J}\dot{\hat{\boldsymbol{\omega}}}_r + (L_J(\hat{\boldsymbol{\omega}}, \mathbf{J}) - L_J(\tilde{\boldsymbol{\omega}}, \mathbf{J}))\hat{\boldsymbol{\omega}}_r \tag{38}$$

where L_J is an operator defined by (62).

We now use (37-38) to propose the following approximation to the ideal controller in (34)

$$\boldsymbol{\tau} = -\mathbf{g}_2 + \mathbf{J}\mathbf{a}_r + L_J(\hat{\boldsymbol{\omega}}, \mathbf{J})\hat{\boldsymbol{\omega}}_r - \mathbf{A}_s\mathbf{J}\mathbf{s} \tag{39}$$

For the theoretical analysis the control in (39) can be written as

$$\boldsymbol{\tau} = \boldsymbol{\tau}_{\text{ideal}} - \mathbf{J}\boldsymbol{\delta}_D + L_J(\tilde{\boldsymbol{\omega}}, \mathbf{J})\hat{\boldsymbol{\omega}}_r \tag{40}$$

Both $\boldsymbol{\delta}_D$ and $L_J(\tilde{\boldsymbol{\omega}}, \mathbf{J})$ converge to zero as the observer error for the angular velocity converges to zero.

By defining $\mathbf{z}_1 = \mathbf{J}\mathbf{s}$ and $\mathbf{w}_1 = -\mathbf{J}\boldsymbol{\delta}_D + L_J(\tilde{\omega}, \mathbf{J})\hat{\omega}_r$ the closed loop dynamics become

$$\dot{\mathbf{z}}_1 = -\mathbf{A}_s \mathbf{z}_1 + \mathbf{w}_1 \quad (41)$$

One may also remove $\mathbf{g}_2$ from (39) and instead add it to $\mathbf{w}_1$, since also $\mathbf{g}_2$ converge to 0 under Ass. 1.

Use of the Lyapunov function $V_z = \frac{1}{2}\mathbf{z}_1^T \mathbf{z}_1$ and the theorem about uniform ultimated boundedness, [24, Th. 4.18], gives that

$$||\mathbf{z}_1||_\infty \leq \max\{\beta_z(|\mathbf{z}_0|, t - t_0), \frac{||\mathbf{w}_1||_\infty}{A_{sm}}\} \quad (42)$$

where β_z is a class-$\mathcal{KL}$ function and A_{sm} is the smallest eigenvalue of $\mathbf{A}_s$. It is possible to choose $\beta_z(|\mathbf{z}_{10}|, 0) \leq |\mathbf{z}_{10}|$, since if $|\mathbf{z}_{10}| \geq \frac{||\mathbf{w}_1||_\infty}{A_{sm}}$ it can be seen that V_z decreases, which implies $|\mathbf{z}_1| < |\mathbf{z}_{10}|$. Using time invariance and the bound on $||\mathbf{z}_1||_\infty$ it can be shown from (42) that

$$||\mathbf{z}_1||_a = \frac{||\mathbf{w}_1||_a}{A_{sm}} \quad (43)$$

see [25, p. 1258]. We know from the analysis of the observer that $||\mathbf{w}_1||_a = 0$, and therefore we have now shown that $||\mathbf{z}_1||_a = 0$, which implies $||\mathbf{s}||_a = 0$ since J is nonsingular.

We now return to the analysis of (33). We have just shown that the dynamics of s is asymptotically stable and from the analysis of the observer we also have that $\mathbf{v}_O \to 0$ as $t \to \infty$. This together with Th. 3 gives the following result:

Theorem 2: If the controller given by (39) with $\boldsymbol{\alpha}_1(\mathbf{e})$ as defined in Th. 3 is applied to the system (28-29), and the states of the leader and follower are estimated by an observer satisfying Ass. 1, then $\mathbf{e} \to \pm\mathbf{1}_q$ for any initial value such that $|\mathbf{e}_0| = 1$. This implies global asymptotic stability of $\mathbf{R}(\mathbf{e}) = \mathbf{I}$.

We have $\mathbf{e} = \hat{\mathbf{e}}_l$ for the tracking problem of the leader and $\mathbf{e} = \hat{\mathbf{e}}_f$ for the synchronization problem of the follower, but are mainly interested in showing that $\mathbf{e}_l \to \pm\mathbf{1}_q$ and $\mathbf{e}_f \to \mathbf{1}_q$. Fig. 1 shows that

$$\mathbf{e}_l = \hat{\mathbf{e}}_l \otimes \tilde{\mathbf{q}}_l^{-1} \quad (44)$$

$$\mathbf{e}_f = \tilde{\mathbf{q}}_l \otimes \hat{\mathbf{e}}_f \otimes \tilde{\mathbf{q}}_f^{-1} \quad (45)$$

This implies that as $\hat{\mathbf{e}}_l$, $\hat{\mathbf{e}}_f$, $\tilde{\mathbf{q}}_l$ and $\tilde{\mathbf{q}}_f$ converge to $\pm\mathbf{1}_q$ also $\mathbf{e}_l$ and $\mathbf{e}_f$ converge to $\pm\mathbf{1}_q$.

VII. Analysis of the attitude error

From the analysis in the last section it is seen that the differential equation for the attitude error is given by (33):

$$\dot{\mathbf{e}} = \frac{1}{2}[\boldsymbol{\alpha}_1(\mathbf{e}) + \Delta\boldsymbol{\omega}]_q \otimes \mathbf{e} \text{ with } \Delta\boldsymbol{\omega} = \mathbf{R}_1^T(\mathbf{s} + \mathbf{v}_O) \quad (46)$$

In this section possible choices of $\boldsymbol{\alpha}_1$ are given such that $\mathbf{e} \to \pm\mathbf{1}_q$ as $t \to \infty$ if $\Delta\boldsymbol{\omega} \to 0$. If $||\Delta\boldsymbol{\omega}||_\infty$ is smaller than a value defined later and $|\boldsymbol{\epsilon}_{e_0}| < 1$ we in addition find a bound for $||\boldsymbol{\epsilon}_e||_\infty$ which is smaller than the a priori bound of 1.

The following Lemma is a well known fact which will be used in the analysis

Lemma 1: For any $\boldsymbol{\omega}_e := \boldsymbol{\alpha}_1(\mathbf{e}) + \Delta\boldsymbol{\omega}$ (46) gives that if the initial value $|\mathbf{e}_0| = 1$ we get $|\mathbf{e}| = 1\ \forall t$, and therefore $\eta_e^2 \leq 1\ \forall t$ and $|\boldsymbol{\epsilon}_e|^2 \leq 1\ \forall t$.

Proof: By differentiating $l_x := \eta_e^2 + \boldsymbol{\epsilon}_e^T\boldsymbol{\epsilon}_e = |\mathbf{e}|^2$ along the trajectories of (46) we get

$$\dot{l}_x = 2\eta_e(-\frac{1}{2}\boldsymbol{\omega}_e^T\boldsymbol{\epsilon}_e) + 2\boldsymbol{\epsilon}_e^T\frac{1}{2}[\eta_e\boldsymbol{\omega}_e - S(\boldsymbol{\epsilon}_e)\boldsymbol{\omega}_e] = 0 \quad (47)$$

and therefore l_x is constant. ■

We always have $|\mathbf{e}_0| = 1$ because it is a unit quaternion from the definition of $\mathbf{e}_0$.

The following Theorem defines some possible choices of $\boldsymbol{\alpha}_1(\mathbf{e})$:

Theorem 3: Let $V(u)$ be a strictly increasing function defined on $[0, 1]$ and let $V(0) = 0$. Assume that V has a bounded derivative such that

$$k_1 \leq \frac{dV(u)}{du} \leq k_2 \quad (48)$$

for all $u \in [0, 1]$.

Define

$$H_\alpha = V(u_e) \text{ with } \quad u_e := 1 - \sqrt{1 - |\boldsymbol{\epsilon}_e|^2} = 1 - |\eta_e| \quad (49)$$

We can look at H_α either as a function of $|\boldsymbol{\epsilon}_e|$ or as a function of η_e. A possible choice of H_α is given by (21), which comes from the choice $V(u) = u$. Let $\boldsymbol{\alpha}_1$ in (46) be chosen as

$$\boldsymbol{\alpha}_1(\mathbf{e}) = \frac{dH_\alpha}{d\eta_e}\boldsymbol{\Lambda}_1\boldsymbol{\epsilon}_e \quad (50)$$

with $\boldsymbol{\Lambda}_1 = \boldsymbol{\Lambda}_1^T > 0$. We have that

$$\frac{dH_\alpha}{d\eta_e} = -sgn(\eta_e)\frac{dV(u_e)}{du_e} \quad (51)$$

The above definition of $\boldsymbol{\alpha}_1$ and (46) implies that if $|\Delta\boldsymbol{\omega}| \to 0$ as $t \to \infty$ then $\mathbf{e} \to \pm\mathbf{1}_q$. Since both $\mathbf{e} = \mathbf{1}_q$ and $\mathbf{e} = -\mathbf{1}_q$ correspond to the rotation matrix $\mathbf{R}_e = I$ there is no attitude error as $t \to \infty$.

Proof: Because $\eta_e^2 + |\boldsymbol{\epsilon}_e|^2 = 1$ for all time we can use only $|\boldsymbol{\epsilon}_e|$ or only $|\eta_e|$ in the analysis. We will look at H_α as a function of $|\boldsymbol{\epsilon}_e|$ because H_α is a positive definite function of $|\boldsymbol{\epsilon}_e|$, and can therefore be used as a Lyapunov function. However, it is a decreasing function of $|\eta_e|$. We have that

$$\dot{H}_\alpha = \frac{dH_\alpha}{d|\boldsymbol{\epsilon}_e|}\frac{d|\boldsymbol{\epsilon}_e|}{dt} = \frac{dH_\alpha}{d\eta_e}\dot{\eta}_e \quad (52)$$

Although we look at H_α as a function of $|\boldsymbol{\epsilon}_e|$ we will calculate the derivative by the last expression in (52), because this is somewhat simpler.

Because we have $|\mathbf{e}| = 1\ \forall t$ from Lemma 1 we know that $u_e \leq 1\ \forall t$ which implies $H_\alpha \leq V(1)\ \forall t$. Define

$$||\Delta\boldsymbol{\omega}||_{[t_1,\infty\rangle} = sup_{t\in[t_1,\infty\rangle}|\Delta\boldsymbol{\omega}| \quad (53)$$

From the assumption $|\Delta\boldsymbol{\omega}| \to 0$ as $t \to 0$ we have that $||\Delta\boldsymbol{\omega}||_{[t_1,\infty\rangle} \to 0$ as $t_1 \to 0$.

For $t \geq t_1$ where t_1 is any time larger than the initial time t_0 we get from (46), (50) and (2) :

$$\dot{H}_\alpha = \frac{dH_\alpha}{d\eta_e}\left\{-\frac{1}{2}\boldsymbol{\epsilon}_e^T\left(\frac{dH_\alpha}{d\eta_e}\boldsymbol{\Lambda}_1\boldsymbol{\epsilon}_e + \Delta\boldsymbol{\omega}\right)\right\} \quad (54)$$

$$\leq -\frac{1}{2}|\boldsymbol{\epsilon}_e|(k_1^2\Lambda_{1m}|\boldsymbol{\epsilon}_e| - k_2||\Delta\boldsymbol{\omega}||_{[t_1,\infty\rangle}) \quad (55)$$

We see that $\dot{H}_\alpha \leq -W_H(|\boldsymbol{\epsilon}_e|)$ where W_H is a positive definite function if

$$|\boldsymbol{\epsilon}_e| > \frac{k_2||\Delta\boldsymbol{\omega}||_{[t_1,\infty\rangle}}{k_1^2\Lambda_{1m}} := \mu_{t_1} \quad (56)$$

Choose t_1 so large that $\mu_{t_1} < 1$. This is possible because of the assumption $||\Delta\boldsymbol{\omega}||_{[t_1,\infty\rangle} \to 0$ as $t_1 \to \infty$. For $\mu_{t_1} > 1$ (56) is never satisfied because $|\boldsymbol{\epsilon}_e| \leq 1$. We know that $H_\alpha \leq V(1)\ \forall t$, and therefore H_α is bounded for $t = t_1$, and we can start the analysis at t_1 instead of at t_0. Since

$$H_\alpha(|\boldsymbol{\epsilon}_e|) > H_\alpha(\mu_{t_1}) \Rightarrow |\boldsymbol{\epsilon}_e| > \mu_{t_1} \quad (57)$$

we have that $\dot{H}_\alpha \leq -W_H(|\boldsymbol{\epsilon}_e|)$ for $H_\alpha(|\boldsymbol{\epsilon}_e|) > H_\alpha(\mu_{t_1})$, and therefore H_α decreases until ultimately

$$H_\alpha(|\boldsymbol{\epsilon}_e|) \leq H_\alpha(\mu_{t_1}) \Rightarrow |\boldsymbol{\epsilon}_e| \leq \mu_{t_1} \quad (58)$$

The arguments above are from [24, Th. 4.18]. By letting $t_1 \to \infty$ in the above analysis we get $\mu_{t1} \to 0$ and therefore $|\boldsymbol{\epsilon}_e| \to 0$, which by using $|\mathbf{e}| = 1$ implies $\eta_e \to \pm 1$, and therefore $\mathbf{e} \to \pm \mathbf{1}_q$. ■

If $||\Delta\boldsymbol{\omega}||_\infty$ and $|\boldsymbol{\epsilon}_{e_0}|$ are small we can find a smaller bound than 1 for $|\boldsymbol{\epsilon}_e|$ during the transient response, by using the following theorem:

Theorem 4: If

$$\mu_{t_0} := \frac{k_2||\Delta\boldsymbol{\omega}||_\infty}{k_1^2\Lambda_m} < 1 \quad (59)$$

and $|\boldsymbol{\epsilon}_{e_0}| < 1$ we have $||\boldsymbol{\epsilon}_e||_\infty < 1$ and satisfying

$$||\boldsymbol{\epsilon}_e||_\infty \leq \max\{|\boldsymbol{\epsilon}_{e_0}|, \mu_{t0}\} \quad (60)$$

Proof: From the proof of Th. 3 with $t_1 = t_0$ we get that if we start with $|\boldsymbol{\epsilon}_{e0}| \leq \mu_{t_0}$ this will be satisfied for all time, because as soon as $|\boldsymbol{\epsilon}_{e0}|$ becomes a bit larger than μ_{t_0} it will decrease. If $|\boldsymbol{\epsilon}_{e0}| > \mu_{t_0}$ we will have $\dot{H}_\alpha < 0$ until $|\boldsymbol{\epsilon}_{e0}| \leq \mu_{t_0}$, and this implies that for $|\boldsymbol{\epsilon}_{e0}| > \mu_{t_0}$ $H_\alpha(|\boldsymbol{\epsilon}_e|) < H_\alpha(|\boldsymbol{\epsilon}_{e_0}|) \Leftrightarrow |\boldsymbol{\epsilon}_e| \leq |\boldsymbol{\epsilon}_{e_0}|$. This implies the bound in (60). ■

VIII. Simulation

A simulation was performed in order to validate the method. The inertia matrices were set to $J_l^l = J_f^f = \mathrm{diag}(5.3, 6.0, 6.7)$. The observer gains for the observer in Sec. V were $K_{v,l} = K_{v,f} = 2\mathbf{I}$ and $k_{p,l} = k_{p,f} = 0.7$. The function $\boldsymbol{\alpha}_1(\mathbf{e})$ was defined as in (50) for both the leader and the follower with $\boldsymbol{\Lambda}_1 = 0.5\mathbf{I}$ for both. The control input was as in (39) with $\mathbf{A}_s = 0.5\mathbf{I}$ for both the leader and the follower, but without the $\mathbf{g}_2$ term as explained below (39). The gains were chosen so low because low available torque has been assumed, since the maximum available torque from thrusters and reaction wheels is mostly not higher than 0.05 Nm for small satellites.

Band-limited white noise was added to the measurements of the attitudes in order to simulate measurement noise. This was done by adding band-limited white noise with standard deviation $\sigma = 0.01$ to each component of $\boldsymbol{\epsilon}$ and calculating η with noise as $\eta_n = \sqrt{1 - \boldsymbol{\epsilon}_n^T\boldsymbol{\epsilon}_n}$, where $\boldsymbol{\epsilon}_n$ is the vector part of the quaternion after noise is added. Since $2\arcsin(0.01) \approx 1^\circ$, this corresponds with an error of about

	η	ϵ_1	ϵ_2	ϵ_3	ω_1	ω_2	ω_3
L	0.4	0.62	0.35	0.5771	$1e-4$	$5e-5$	$3e-4$
LO	0.4	0.62	0.35	0.5771	0	0	0
F	0.2	0.8	0.5	0.2646	$2e-4$	$4e-4$	$15e-4$
FO	0.2	0.8	0.5	0.2646	0	0	0

TABLE I

Initial values, L: Leader, LO: Observer for the leader, F: Follower, FO: Observer for the follower.

1° in the measurement of angles. The noise was different on each element.

The desired attitude for the leader was given by $\mathbf{q}_d(t) = \mathbf{q}_1 \otimes \tilde{\mathbf{q}}_1(t)$ with $\mathbf{q}_1 = [\ 0.3 \quad 0.7 \quad 0.4 \quad 0.5099\ ]^T$ and $\tilde{\mathbf{q}}_1(t) = [\ \cos(\frac{\theta(t)}{2}) \quad \sin(\frac{\theta(t)}{2})\mathbf{k}^T]^T$. The rotation axis $\mathbf{k}$ was constant and defined by $\mathbf{k}^T = [\ 0.1574 \quad 0.9861 \quad -0.0551\ ]$ and $\theta(t) = \frac{\theta_M}{T_\theta}e^{-\frac{t}{T_\theta}}$ with $\theta_M = \pi/3$ and $T_\theta = 60$ seconds.

The initial values are shown in table I. We assume that the synchronization scheme starts after detumbling of the satellites, and therefore it is known that the initial angular velocity of each satellite is small.

In Fig. 3 the results for the quaternion elements of the desired attitude, the leader attitude and the follower attitude are shown. The control torque varied between ± 0.02 Nm after the transient response, and between ± 0.15 Nm during the transient response. In order to have torques smaller than ± 0.05 Nm all the time one would therefore have to use smaller gains during the transient response, and the response would then take longer time.

Before $t = 55$ seconds the attitudes are plotted without the added noise, since we want to see how well the actual trajectories converge to each other.

In Fig. 4 the rotation angle corresponding with the tracking error $\mathbf{e}_l$ for the leader, and synchronization error $\mathbf{e}_f$ for the follower is shown after the transient response. It was calculated by $\theta_k = 2\arcsin(\sqrt{\boldsymbol{\epsilon}_{e_k}^T\boldsymbol{\epsilon}_{e_k}})$ for $k = l, f$. The angle is higher for the synchronization than for the tracking, but we see that in both cases the angle is small. It was seen that $\mathbf{e}_l \approx \mathbf{1}_q$ and $\mathbf{e}_f \approx \mathbf{1}_q$. With other initial values we got convergence to $-\mathbf{1}_q$.

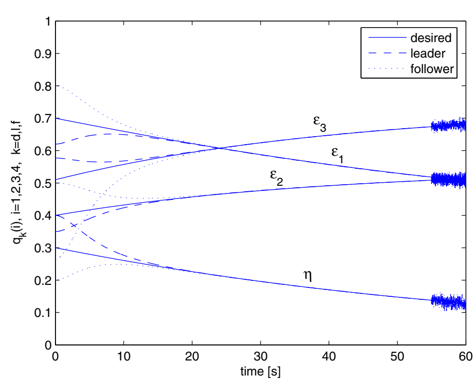

Fig. 3. Quaternion elements for the desired attitude, leader and follower . Before $t = 55$ minutes the attitudes are plotted without the added noise

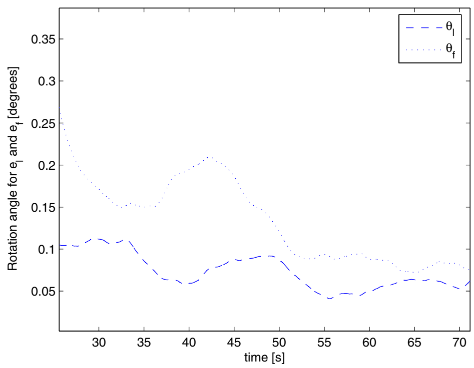

Fig. 4. Rotation angle corresponding with $\mathbf{e}_l$ and $\mathbf{e}_s$, calculated from the actual values (before the noise is added).

IX. Conclusion

A scheme for output feedback synchronization of the attitude of two satellites was developed, and the results were validated by simulation. It was shown by analysis that the rotation matrix for the attitude error converges to the identity matrix for any initial values. This was confirmed by the simulations.

Appendix
Deduction of an approximation to $\dot{\hat{\boldsymbol{\omega}}}_{il}^i$

We have

$$\begin{aligned}\dot{\mathbf{J}}_l^i &= \frac{d}{dt}(\mathbf{R}_l\mathbf{J}_l^l\mathbf{R}_l^T) = \mathbf{S}(\boldsymbol{\omega}_{il}^i)\mathbf{J}_l^i - \mathbf{J}_l^i\mathbf{S}(\boldsymbol{\omega}_{il}^i) \\ &= \mathbf{S}(\hat{\boldsymbol{\omega}}_{il}^i - \tilde{\boldsymbol{\omega}}_{il}^i)\mathbf{J}_l^i - \mathbf{J}_l^i\mathbf{S}(\hat{\boldsymbol{\omega}}_{il}^i - \tilde{\boldsymbol{\omega}}_{il}^i) \end{aligned} \tag{61}$$

By defining the operator

$$L_J(\boldsymbol{\omega}, \mathbf{J}) = \mathbf{S}(\boldsymbol{\omega})\mathbf{J} - \mathbf{J}\mathbf{S}(\boldsymbol{\omega}) \tag{62}$$

(61) becomes

$$\dot{\mathbf{J}}_l^i = L_J(\hat{\boldsymbol{\omega}}_{il}^i, \mathbf{J}_l^i) - L_J(\tilde{\boldsymbol{\omega}}_{il}, \mathbf{J}_l^i) \tag{63}$$

where the first term is known and the second term goes to zero as the observer errors go to zero. From

$$\begin{aligned}&\frac{d}{dt}(\mathbf{J}_l^i\hat{\boldsymbol{\omega}}_{il}^i) = \boldsymbol{\tau}_l^i + \mathbf{g}_{2m} \\ &\mathbf{J}_l^i\dot{\hat{\boldsymbol{\omega}}}_{il}^i + (L_J(\hat{\boldsymbol{\omega}}_{il}^i, \mathbf{J}_l^i) - L_J(\tilde{\boldsymbol{\omega}}_{il}, \mathbf{J}_l^i))\hat{\boldsymbol{\omega}}_{il}^i = \boldsymbol{\tau}_l^i + \mathbf{g}_{2l} \end{aligned} \tag{64}$$

we get $\dot{\boldsymbol{\omega}}_D = \dot{\hat{\boldsymbol{\omega}}}_{il}^i = \mathbf{a}_D + \boldsymbol{\delta}_D$ with

$$\mathbf{a}_D = (\mathbf{J}_l^i)^{-1}\left\{\boldsymbol{\tau}_l^i + \mathbf{g}_{2l} - L_J(\hat{\boldsymbol{\omega}}_{il}^i, \mathbf{J}_l^i)\hat{\boldsymbol{\omega}}_{il}^i\right\} \tag{65}$$

$$\boldsymbol{\delta}_D = (\mathbf{J}_l^i)^{-1}L_J(\tilde{\boldsymbol{\omega}}_{il}^i, \mathbf{J}_l^i)\hat{\boldsymbol{\omega}}_{il}^i \tag{66}$$

References

[1] D. Scharf, F. Hadaegh, and S. Ploen, "A survey of spacecraft formation flying guidance and control (part II): Control," in *Proccedings of the 2004 American Control Conference*, Boston, MA, 2004, pp. 2976–2985.

[2] P. K. C. Wang and F. Hadaegh, "Coordination and control of multiple microspacecraft moving in formation," *The Journal of the Astronautical Sciences*, vol. 44, pp. 315–355, 1996.

[3] P. Wang, F. Hadaegh, and K. Lau, "Syncronized formation rotation and attitude control of multiple free-flying spacecraft," *Journal of guidance, control and dynamics*, vol. 22, no. 1, pp. 28–35, 1999.

[4] R. W. Beard, J. Lawton, and F. Y. Hadaegh, "C coordination architecture for spacecraft formation control," *IEEE Transactions on control systems technology*, vol. 9, pp. 777–790, November 2001.

[5] J. T.-Y. Wen and K. Kreutz-Delgado, "The attitude control problem," *IEEE Transactions on automatic control*, vol. 36, no. 10, pp. 1148–1162, 1991.

[6] H. Pan and V. Kapila, "Adaptive nonlinear control for spacecraft formation flying with coupled translational and attitude dynamics," in *Proceedings of the 40th IEEE Conference on Decision and Control*, Orlando, Fl, 2001, pp. 2062–2067.

[7] B. Costic, D. Damon, M. de Queiroz, and V. Kapilia, "A quaternion-based adaptive attitude tracking controller without velocity measurements," in *Proceedings of the 39th IEEE Conference on Decision and Control*, Sydney, Australia, 2000, pp. 2429–2434.

[8] Q. Yan, G. Yang, V. Kapila, and M. de Queiroz, "Nonlinear dynamics and output feedback control of multiple spacecraft in elliptical orbits," in *Proceedings of the American Control Conference*, Chicago, Illinois, 2000, pp. 839–843.

[9] F. Lizarralde and J. T. Wen, "Attitude control without angular velocity measurement: a passivity approach," *IEEE Transactions on automatic control*, vol. 41, no. 3, pp. 468–472, March 1996.

[10] J. Lawton and R. Beard, "Synchronized multiple spacecraft rotations," *Automatica*, vol. 38, pp. 1359–1364, 2002.

[11] W. Kang, N. Xi, and A. Sparks, "Theory and applications of formation control in a perceptive reference frame," in *Proceceedings of the 39th IEEE Conference on Decision and Control*, Sydney, Australia, 2000, pp. 352–357.

[12] W. Kang and H.-H. Yeh, "Co-ordinated attitude control of multi-satellite systems," *International journal of robust and nonlinear control*, vol. 12, pp. 185–205, 2002.

[13] K. Köprübasi and M.-W. L. Thein, "Spacecraft attitude and rate estimation using sliding mode observers," in *Proceedings of International Conference on Recent Advances in Space Technologies*, 2003, pp. 169–173.

[14] J. B. Kuipers, *Quaternions and rotation sequences*. Princeton university press, Princeton, New Jersey, 1999.

[15] O. Egeland and J. T. Gravdahl, *Modelling and Simulation for Automatic Control*. Marine Cybernetics, Trondheim, Norway, 2002.

[16] S. Salcudean, "A globally convergent angular velocity observer for rigid body motion," *IEEE Transactions on automatic control*, vol. 36, no. 12, pp. 1493–1497, 1991.

[17] O.-E. Fjellstad, "Control of unmanned underwater vehicles in six degrees of freedom: a quaternion feedback approach," Doktor Ingeniøravhandling, Report 94-92-W, Department of Engineering Cybernetics, The Norwegian institute of Technology, University of Trondheim, Norway, November 1994.

[18] T. I. Fossen and Å. Grøvlen, "Nonlinear output feedback control of dynamically positioned ships using vectorial observer backstepping," *IEEE Transactions on control systems technology*, vol. 6, no. 1, pp. 121–128, 1998.

[19] M. Krstic, I. Kanellakopoulos, and P. Kokotovic, *Nonlinear and Adaptive Control Design*. John Wiley & Sons., Inc., 1995.

[20] A. Robertsson and R. Johansson, "Comments on "nonlinear output feedback control of dynamically positioned ships using vectorial observer backstepping*"," *IEEE Transactions on control systems technology*, vol. 6, no. 3, pp. 439–441, 1998.

[21] M.-H. Kim and D. J. Inman, "Development of a robust non-linear observer for dynamic positioning of ships," *Proceedings of the institution of mechanical engineers part I - Journal of systems and control engineering*, vol. 218, no. 1, pp. 1–11, 2004.

[22] J. Lu and B. Wie, "Nonlinear quaternion feedback control for spacecraft via angular velocity shaping," 1994, proceedings of the American Control Conference, Baltimore, Maryland.

[23] A. K. Bondhus, K. Y. Pettersen, and H. Nijmeijer, "Master-slave synchronization of robot manipulators," 2004, iFAC Symposium NOLCOS 2004, Symposium on Nonlinear Control Systems.

[24] H. H. Khalil, *Nonlinear Systems*, 3rd ed. Prentice Hall, 2002.

[25] A. R. Teel, "A nonlinear small gain theorem for the analysis of control systems with saturation," *IEEE Transactions on Automatic Control*, vol. 41, no. 9, pp. 1256–1270, September 1996.